Recombinant Soluble Human $\alpha_3\beta_1$ Integrin: Purification, Processing, Regulation, and Specific Binding to Laminin-5 and Invasin in a Mutually Exclusive Manner†

Johannes A. Eble,*,‡ Kai W. Wucherpfennig,‡ Laurent Gauthier,‡ Petra Dersch,§ Eric Krukonis,§ Ralph R. Isberg,§ and M. E. Hemler‡

Dana Farber Cancer Institute, Harvard Medical School, 44 Binney Street, Boston, Massachusetts 02115, and Department of Microbiology and Molecular Biology, Howard Hughes Medical Institute, Tufts University, School of Medicine, Boston, Massachusetts 02111

Received January 23, 1998; Revised Manuscript Received May 18, 1998

ABSTRACT: Using insect cells, we expressed large quantities of soluble human integrin $\alpha_3\beta_1$ ectodomain heterodimers, in which cytoplasmic and transmembrane domains were replaced by Fos and Jun dimerization motifs. In direct ligand binding assays, soluble $\alpha_3\beta_1$ specifically bound to laminin-5 and laminin-10, but not to laminin-1, laminin-2, fibronectin, various collagens, nidogen, thrombospondin, or complement factors C3 and C3b. Soluble $\alpha_3\beta_1$ integrin also bound to invasin, a bacterial surface protein, that mediates entry of *Yersinia* species into the eukaryotic host cell. Invasin completely displaced laminin-5 from the $\alpha_3\beta_1$ integrin, suggesting sterically overlapping or identical binding sites. In the presence of 2 mM Mg^{2+}, $\alpha_3\beta_1$'s binding affinity for invasin ($K_d = 3.1$ nM) was substantially greater than its affinity for laminin-5 ($K_d > 600$ nM). Upon addition of 1 mM Mn^{2+}, or activating antibody 9EG7, binding affinity for both laminin-5 and invasin increased by about 10-fold, whereas the affinity decreased upon addition of 2 mM Ca^{2+}. Thus, functional regulation of the purified soluble integrin $\alpha_3\beta_1$ ectodomain heterodimer resembles that of wild-type membrane-anchored β_1 integrins. The integrin α_3 subunit was entirely cleaved into disulfide-linked heavy and light chains, at a newly defined cleavage site located C-terminal of a tetrabasic RRRR motif. Within the α_3 light chain, all potential N-glycosylation sites bear N-linked mannose-rich carbohydrate chains, suggesting an important structural role of these sugar residues in the stalk-like region of the integrin heterodimer. In conclusion, studies of our recombinant $\alpha_3\beta_1$ integrin have provided new insights into $\alpha_3\beta_1$ structure, ligand binding function, specificity, and regulation.

The integrin family contains 22 distinct cell surface $\alpha\beta$ heterodimers that contribute to cell−cell and cell−matrix interactions (for reviews, see refs *1* and *2*). Both the α and the β subunits consist of a large extracellular domain with N-terminal halves that bind divalent cations and ligands. As determined by electron microscopy, the globular N-terminal halves and the stalk-like C-terminal regions of both ectodomains, along with the short transmembrane and cytoplasmic tails, give the integrin a mushroom-like shape (*3*). Some integrin α subunits, e.g., α_3, α_6, and α_7, are proteolytically cleaved within this stalk-like region to yield disulfide-linked heavy and light chains. The ectodomains of both integrin subunits are anchored within the cell membrane by α helical transmembrane domains. Regulated by the cytoplasmic tail of the α subunit, the cytoplasmic domain of the β subunit interacts with the cytoskeleton (*4*, *5*). By linking the extracellular matrix with the intracellular cytoskeleton, integrins allow physical forces and biological signals to be transferred between the cell and its surroundings.

Among the 22 $\alpha\beta$ heterodimers, $\alpha_3\beta_1$ is particularly interesting because of its role in development and other biological processes, such as tumorigenesis (*6*) and wound healing (*7*). Mice deficient in α_3 die shortly after birth with malformation of the kidney and lung. The $\alpha_3\beta_1$ integrin may be involved in tubule branching which is characteristic of these two organs, and in the organization of the basal membrane (*8*). Also demonstrating the pivotal role of $\alpha_3\beta_1$ integrin in the establishment and maintanance of the basal membrane, DiPersio et al. (*9*) found matrix disorganization and concomitant blistering at the dermal−epidermal junction in the skin of α_3-deficient mice. The $\alpha_3\beta_1$ integrin is abundant on keratinocytes in the basal layer of the skin epidermis. These epithelial cells form close contacts with the basal membrane, and in particular with the anchoring filaments, mainly consisting of laminin-5 (also called kalinin, epiligrin, or nicein) (*10*, *11*). During wound healing, laminin-5 expression in skin wounds is increased, and during re-epithelization, keratinocytes migrate into the wound bed by using the $\alpha_3\beta_1$ integrin (*7*). The anchoring filaments of laminin-5 reach into the *lamina densa* of the basal membrane, which is formed by the dense network of type IV collagen,

† This work was supported by fellowships from the Deutsche Forschungsgemeinschaft to J.A.E. (Eb 177/1-1) and to P.D. (De 616/1-2) and by National Institutes of Health Grant CA42368 (to M.E.H.). J.A.E. currently receives an Otto-Hahn fellowship of the Max-Planck-Gesellschaft zur Förderung der Wissenschaften.

* To whom correspondence should be addressed. Current address: Institut für Physiologische Chemie und Pathobiochemie, Westfälische Wilhelms-Universität Münster, Waldeyerstrasse 15, 48149 Münster, Germany. Phone: ++49-251-835 5570. Fax: ++49-251-835 5596. E-mail: eble@uni-muenster.de.

‡ Harvard Medical School.

§ Tufts University.

S0006-2960(98)00175-5 CCC: $15.00
Published on Web 07/11/1998

laminin isoforms other than laminin-5, nidogen/entactin, perlecan, and other extracellular matrix proteins (*12*).

Ligands proposed for $\alpha_3\beta_1$ integrin include collagen, fibronectin (*13*, *14*), laminin (*15*−*17*), nidogen/entactin (*18*), and thrombospondin (*19*). A pathogenic ligand for $\alpha_3\beta_1$ is invasin, a bacterial surface protein responsible for the attachment of *Yersinia* to eukaryotic host cells (*20*). The cell- and integrin-binding domain is located within the 192 C-terminal amino acids of invasin (*21*). In many cases, extracellular matrix ligands for $\alpha_3\beta_1$ have been defined using assays of cell adhesion, a complex multistep phenomenon. The primary event of $\alpha_3\beta_1$-mediated cell attachment, i.e., the protein−protein interaction of the $\alpha_3\beta_1$ integrin with its respective ligand, has not been studied well, largely because of difficulties with soluble ligand binding studies using putative $\alpha_3\beta_1$ ligands. Also, the $\alpha_3\beta_1$ integrin itself has previously not been isolated in amounts necessary for definitive cell-free ligand binding assays.

To study the interaction of $\alpha_3\beta_1$ integrin with the basal membrane constituents and other extracellular matrix proteins, large quantities of pure $\alpha_3\beta_1$ integrin are required. Here we report the synthesis of recombinant soluble human $\alpha_3\beta_1$ integrin with an insect cell expression system, the purification of $\alpha_3\beta_1$ using the immobilized integrin-binding domain of invasin, characterization of glycosylation and endoproteolytic cleavage of the purified protein, and the results of direct ligand binding studies carried out with recombinant soluble $\alpha_3\beta_1$ integrin in a defined cell-free system.

EXPERIMENTAL PROCEDURES

Construction of Expression Vectors pUC-hygMT-a3-Fos and pUC-hygMT-β_1-Jun. cDNAs of α_3-Fos, encoding the human integrin α_3 ectodomain fused to the dimerizing α helix of the transcription factor Fos, were prepared by using a two-step PCR protocol. In the first step, using pKS+-α_3WT cDNA (*22*) as a template, a 575 bp fragment was generated, spanning from an internal α_3 *Avr*II site through codons for the last amino acids of the α_3 ectodomain (LPAEIE), with an added sequence encoding a GGSTGGG spacer and the first few amino acids (LTDTL) of the Fos α helical sequence. The forward primer A3F3 (32 bp) was 5′-GAC CCT GGT CCT AGG TCT GGA GTG GCC CTA CG-3′ with the *Avr*II site underlined, and the reverse primer A3FosR1 (56 bp) was 5′-GGA GTG TAT CAG TTA AAC CGC CGC CCG TCG ACC CTC CCT CGA TTT CGG CCG GCA GC-3′ with an analytical *Sal*I site underlined. Also, using the Fos α helix containing plasmid pRmHa3fos (*23*) as a template, a 178 bp fragment was generated, beginning with a short sequence encoding the last C-terminal amino acids (LPAEIE) of the α_3 ectodomain and a sequence encoding the GGSTGGG spacer and the entire Fos α helix sequence and ending with an *Xba*I site after a stop codon. The forward primer A3FosF1 (56 bp) was antiparallel and complementary to the above-described reverse primer A3FosR1, and the reverse primer FosR1 (46 bp) was 5′-CCC GAG ATC TAG ACG CGC GGA TCC TCA GTG GGC GGC CAG GAT GAA C-3′ with the *Xba*I site underlined. In the second PCR step, the outer primers, A3F3 (32 bp) and FosR1 (46 bp), and the 578 and 178 bp fragments were used to prepare a cDNA fragment of 697 bp. After digestion with *Avr*II and *Xba*I, this fragment was used to replace the respective wild-type sequence of α_3 in the Bluescript plasmid, thus giving rise to the mutant plasmid pKS+-α_3-Fos. Next, using the *Xba*I restriction sites, the entire α_3-Fos sequence was cloned into the insect cell expression vector pUC-hygMT (*23*) under the control of the inducible metallothionin promoter (*24*).

With a similar cloning strategy, cDNA encoding β_1-Jun was prepared, which contains the β_1 ectodomain fused to the dimerizing α helix of the transcription factor Jun. In the first PCR step, using pECE-β_1WT cDNA (*25*) as a template, a 120 bp fragment was generated, spanning from a unique *Sna*BI restriction site within the β_1 coding sequence through a sequence encoding the last amino acids (PECPT-GPD) of the β_1 ectodomain, with an added sequence encoding a GGSAGGG spacer and the first amino acids (RIAR) of the dimerizing Jun α helix. The forward primer B1F1 (37 bp) was 5′-TGG TTC TAT TTT ACG TAT TCA GTG AAT GGG AAC AAC G-3′ with the *Sna*BI site underlined, and the reverse primer B1JunR1 (58 bp) was 5′-GCC GGG CGA TGC GAC CGC CGC CGG CCG ACC CTC CGT CTG GAC CAG TGG GAC ACT CTG G-3′ with an analytical *Nae*I site underlined. Also, using the Jun α helix encoding plasmid pRmHa3jun (*23*) as a template, a 186 bp fragment was generated, using the forward primer B1JunF1 (58 bp), which is antiparallel and complementary to the reverse primer B1JunR1 (58 bp) described above, and the reverse primer JunR1 (49 bp) 5′-GTG TGT TCT AGA GTG AAT TCG TCA GTG GTT CAT GAC TTT CTG TTT AAG C-3′ with the *Xba*I site underlined. In the second PCR step, the outer pair of primers, B1F1 (37 bp) and JunR1 (49 bp), and the 120 and 186 bp fragments were used to prepare a 242 bp cDNA fragment. After digestion with *Sna*BI and *Xba*I, this fragment was used to replace a *Sna*BI−*Xba*I fragment within the pECE-β_1WT vector, thus yielding the mutant pECE-β_1-Jun sequence. Then, the entire β_1-Jun coding sequence was excised with *Sal*I and *Xba*I and directionally inserted into pUC-hygMT to give the pUC-hygMT-β_1-Jun construct. All PCR-derived sequences were verified by DNA sequencing.

Cell Culture and Expression of Human Soluble $\alpha_3\beta_1$. Drosophila Schneider cells were grown at 25 °C in SF900 medium supplemented with 10% fetal calf serum, 100 units/mL penicillin G, and 0.1 mg/mL streptomycin sulfate (Life Technologies, Grand Island, NY). Schneider cells were cotransfected with 8 μg each of pUC-hygMT-α_3-Fos and pUC-hygMT-β_1-Jun, using 18 μL of cellfectin reagent (Life Technologies). Briefly, 8×10^6 cells were plated for 90 min, washed three times with serum-free medium, and then incubated with cellfectin reagent and expression vectors for 5 h. After a 4 day recovery, transfected cells were selected with hygromycin B, added up to 100 μg/mL. A stable clone JAE1.1 was established from a single cell after two rounds of subcloning by limiting dilution, and screening with a sandwich ELISA.

Expression of soluble $\alpha_3\beta_1$ integrin by Schneider cells, grown in spinner flasks to a density of $5-10 \times 10^6$ cells/mL, was optimally induced by addition of 0.8 mM $CuSO_4$. The presence of 10% fetal calf serum facilitated both growth of JAE1.1 cells and $\alpha_3\beta_1$ production. Four to five days after induction, the cell supernatant was harvested after adjusting the mixture so it contained 1 mM EDTA,[1] 1 mM $MgCl_2$, 1 μg/mL aprotinin, 1 μg/mL leupeptin, and 0.04% sodium azide.

Sandwich ELISA. Levels of soluble $\alpha_3\beta_1$ integrin were quantitated by sandwich ELISA (antigen-capture ELISA). The anti-α_3 monoclonal antibody A3-IIF3 (*26*) was coated onto a microtiter plate at 4 °C overnight. Then at room temperature, nonspecific binding sites were blocked for 2 h, using a 1% solution of bovine serum albumin (BSA) in phosphate-buffered saline (PBS). Next, microtiter wells were incubated with the $\alpha_3\beta_1$ solution for 2 h and washed three times with PBS. To detect $\alpha_3\beta_1$ captured by the immobilized A3-IIF5 antibody, microtiter plates were next incubated with a polyclonal rabbit anti-human β_1 antiserum [raised against the human integrin β_1 subunit, purified from human placenta (*27*)], washed, and then incubated with a goat anti-rabbit IgG antibody covalently coupled to alkaline phosphatase (Sigma, St. Louis, MO). Both primary and secondary antibodies were diluted in PBS containing 1% BSA. Finally, *p*-nitrophenyl phosphate (pNpp) was used to detect the bound alkaline phosphatase, and the absorbance at 405 nm was measured in a model 3550 microplate reader (Bio-Rad, Hercules, CA). In a concentration range of 0−160 ng/mL, the sandwich ELISA gave a linear dose-dependent signal. The assay gave similar results in both the absence and presence of EDTA, indicating that the A3-IIF5 epitope on α_3 is not influenced by divalent cations. Also, similar results were obtained when anti-α_3 monoclonal antibodies A3-IIF5, A3-X8, and A3-IVA5 were used as capturing antibodies.

Purification of the Soluble $\alpha_3\beta_1$. After centrifugation and filtering, the insect cell supernatant containing soluble $\alpha_3\beta_1$ integrin was concentrated in a model 2000 Amicon concentrator (Amicon Inc., Beverly, MA) and washed five times with Tris-buffered saline [TBS, 10 mM Tris-HCl (pH 7.4) and 150 mM NaCl] containing 2 mM $MgCl_2$. After 1 mM $MnCl_2$ was added, the concentrate was passed through a column, onto which the fusion protein MBP−invasin had been covalently coupled (described below), and the column was washed with TBS, containing 2 mM $MgCl_2$ and 1 mM $MnCl_2$. The bound $\alpha_3\beta_1$ integrin was eluted with a 20 mM EDTA solution in TBS. After the mixture was supplemented with 30 mM $MgCl_2$, the eluate fractions were concentrated and washed by centrifugation in a Centricon 50 ultrafiltration unit (Amicon Inc.). The concentration of the soluble $\alpha_3\beta_1$ was determined with a BCA (Pierce, Rockford, IL). After electrophoretic separation and blotting onto a PVDF membrane (Bio-Rad), the integrin subunits were N-terminally sequenced by Edman degradation. The α_3-Fos light chain was digested on the membrane with endoproteinase Lys-C, and the eluted fragments were separated on a RP-C8 column using HPLC. The N-terminal fragment was identified by mass spectroscopy and sequenced by Edman degradation after deblocking its N terminus with pyroglutamate aminopeptidase (Takada Biochemicals, Shiga, Japan).

Glycoconjugate Analysis and Cleavage of N-Linked Carbohydrate Chains. Purified, soluble $\alpha_3\beta_1$ integrin was coated at 10 μg/mL onto a microtiter plate at 4 °C overnight. Because antibodies usually contain both N- and O-linked carbohydrate structures, we used the monoclonal antibody A3-IIF5 (also coated at 10 μg/mL) as a positive control. Nonspecific binding sites were blocked for 2 h using 1% heat-inactivated BSA in TBS (pH 7.4) containing 2 mM $MgCl_2$, 1 $MnCl_2$, and 2 mM $CaCl_2$ (TBS/Mg/Mn/Ca buffer), and then various biotinylated lectins (Pierce and Sigma) were applied at a concentration of 10 μg/mL at room temperature for 2 h. After the wells were washed four times with the TBS/Mg/Mn/Ca buffer, the bound lectin was detected by incubation for 1 h with an extravidin−alkaline phosphatase conjugate (Sigma) diluted 1:1000 in the TBS/Mg/Mn/Ca buffer. After four washing steps, alkaline phosphatase activity was measured using pNpp and stopped with a 3 M NaOH solution and the absorbance read at 405 nm. The absorbance measured in the BSA-coated wells was less than 10% relative to maximum absorbance values, and was routinely subtracted.

For digestion with *N*-glycosidase F, recombinant $\alpha_3\beta_1$ integrin was diluted to 0.25 mg/mL in TBS buffer (pH 7.4) containing 2 mM $MgCl_2$. After incubation with *N*-glycosidase F (Boehringer Mannheim, Indianapolis, IN) (75 milliunits/μg of integrin) at 37 °C for 4 h, the same amount of *N*-glycosidase F was added again and the digestion was continued at 37 °C overnight.

Purification of MBP−Invasin (MBP−Inv497) and Construction of the MBP−Invasin Affinity Matrix. To study integrin−invasin interaction, we used MBP−invasin (MBP−Inv497), in which the 497 C-terminal amino acids of invasin containing the integrin-binding domain of invasin were fused to the maltose-binding protein (MBP) (*21*). *Escherichia coli* MC4100 *leu*$^+$ *ara*$^+$ Δ*phoA-Pvu*II*lpp*5508 *degP*::Tn5 (F′*pro*AB$^+$*lacI*q*lacZ*ΔM15) (*28*) cells harboring the plasmid pRI285 encoding the MBP−Inv497 fusion protein were grown at 30 °C in 20 L of 2× YT medium and 100 μg/mL ampicillin until A_{600} equaled 1.0. Then IPTG was added to 1 mM to induce the *lac* promoter, and the culture was grown for an additional 2 h at 30 °C. After being washed in buffer A [10 mM Tris-HCl (pH 8.0), 150 μg/mL PMSF, 0.03 unit/mL of aprotinin, pepstatin, leupeptin, and protease mix (Boehringer Mannheim)], the cells were lysed by three passes through a French press cell at 14 000 psi. After unlysed cells and the insoluble debris were removed by centrifugation, the supernatant was loaded onto a Sepharose Q column (HiLoad 26/10, Pharmacia Biotech Inc., Piscataway, NJ). The column was washed with 300 mL of buffer B [10 mM Tris-HCl (pH 8.0) and 150 μg/mL PMSF]. The MBP−Inv497 fusion protein was eluted using a 300 mL linear salt gradient (0 to 500 mM NaCl) in buffer B. The eluted MBP−Inv497 fusion protein was precipitated with 50% ammonium sulfate, resuspended, and dialyzed against buffer B. To construct the MBP−invasin affinity matrix, approximately 30 mg of the fusion protein was cross-linked to 10 mL of Affi-Gel 10 (Bio-Rad) at a protein concentration of 1 mg/mL following the manufacturer's instructions.

Purification of Laminin-5. Human SSC25 cells, provided by J. Rheinwald (Brigham and Women's Hospital, Boston, MA), were grown for 2 days in a 1:1 mixture of DMEM and F12 media, containing 100 units/mL penicillin G, 0.1 mg/mL streptomycin sulfate, 0.4 μg/mL hydrocortisone, 1 μg/mL aprotinin, and 1 μg/mL leupeptin. After the cell supernatant was harvested, the cells were allowed to recover for 2 days in serum-supplemented medium (10% fetal calf serum). The conditioned medium was filtered and sodium azide added to a final concentration of 0.04%.

[1] Abbreviations: BSA, bovine serum albumin; EDTA, ethylenediaminetetraacetate; MBP, maltose binding protein; PBS, phosphate-buffered saline; pNpp, *p*-nitrophenyl phosphate; TBS, Tris-buffered saline.

The laminin-5 was then purified as described (*10*, *29*). The SSC25-conditioned medium was first passed over a gelatin−Sepharose column to remove fibronectin and then over a 6F12-Sepharose CL-4B affinity column prepared by coupling the anti-laminin-5 β3 chain antibody 6F12 (K140) (*30*) to cyanogen-activated Sepharose CL-4B (Pharmacia Biotech). The 6F12 (K140) hybridoma cells were generously provided by R. Burgeson (Massachusetts General Hospital, Boston, MA). Laminin-5 was eluted from the 6F12 column with a 1 M acetic acid solution, neutralized by addition of 2 M Tris-HCl (pH 8.0), and dialyzed against TBS containing 0.02% sodium azide. The protein concentration was determined with a BCA (Pierce), and the purity was tested by SDS−PAGE.

Other Extracellular Matrix Proteins. Rat tail collagen I was purchased from Sigma. All other collagens were kindly provided by K. Kühn and A. Ries (Max-Planck-Institut für Biochemie, Martinsried, Germany). Collagen III was from calf skin, whereas type IV collagen tetramer, type IV collagen dimer, and collagen V were from human placenta. Type IV collagen dimers and tetramers were extracted from insoluble tissue type IV collagen using two different enzymatic digestions. Together, these two preparations cover the entire type IV collagen molecule (*31*, *32*). All collagens were used in a 0.1 M acetic acid solution, except for the type IV collagen dimer, which was dissolved in TBS. Recombinant nidogen/entactin was a generous gift from R. Timpl (Max-Planck-Institut für Biochemie). To ensure its native conformation, the nidogen/entactin was expressed recombinantly (*33*). Thrombospondin-1 was kindly supplied by J. Lawler (Beth Israel Hospital, Boston, MA). Fibronectin, mouse Engelbreth−Holm−Swarm (EHS) laminin, human laminin-2 (merosin), and human laminin were purchased from Life Technologies. Human placental laminin had been immunopurified with mAb 4C7 after partial pepsin digestion of human placenta. mAb 4C7 recognizes the α5 chain of laminin-10, which is abundant in placental tissue (*34*, *35*; L. Sorokin, personal communication). Therefore, the placental human laminin used in our experiments mainly consists of laminin-10. Human complement proteins C3 and C3b were obtained from Advanced Research Technologies (San Diego, CA).

Binding Tests and Titration Assays. Extracellular matrix proteins (at 20 μg/mL) in TBS (pH 7.4) containing 2 mM $MgCl_2$ (TBS/Mg buffer) were coated onto a microtiter plate at 4 °C overnight. The collagens, with the exception of collagen IV dimers, were coated in 0.1 M acetic acid. Thrombospondin-1 was coated in the TBS/Mg buffer supplemented with 2 mM $CaCl_2$, to ensure its native conformation which is necessary for cell binding. Complement factors C3 and C3b were coated in the TBS/Mg buffer containing 0.08% diethylamine to destroy the intramolecular thioester bond, which might cause nonspecific binding.

After being coated, the plate was washed with the TBS/Mg buffer. Nonspecific binding sites on the plastic surface were blocked with a 1% solution of BSA in the TBS/Mg buffer for 2 h at room temperature. All the following steps were performed at room temperature. Soluble $\alpha_3\beta_1$ integrin was diluted in the TBS/Mg buffer containing 1% BSA, and the mixture was added to ligand-coated microtiter wells for 2 h. To examine the $\alpha_3\beta_1$ ligand spectrum under optimal conditions, $\alpha_3\beta_1$ was applied at a concentration of 100 nM in the presence of 1 mM $MnCl_2$. For titration assays, the concentration of $\alpha_3\beta_1$ was varied, and divalent cations and activating rat mononclonal anti-β_1 antibody 9EG7 (*36*, *37*) (kindly provided by D. Vestweber, Münster, Germany) were added as specified. After the wells were washed three times with 25 mM HEPES (pH 7.6) containing 2 mM $MgCl_2$ and 1 mM $MnCl_2$, the bound receptor was fixed to the plate with 2.5% glutaraldehyde in the same buffer for 10 min. After the wells were washed three times with the TBS/Mg buffer, the amount of bound $\alpha_3\beta_1$ integrin was determined with an ELISA. Rabbit polyclonal anti-human β_1 integrin antiserum was diluted 1:300 in the TBS/Mg buffer containing 1% BSA, and the mixture was incubated for 90 min. After the wells were washed three times with the TBS/Mg buffer, secondary goat anti-rabbit IgG antibody coupled to alkaline phosphatase was applied in a 1:300 dilution in the TBS/Mg buffer containing 1% BSA. When recombinant $\alpha_3\beta_1$ binding was measured in the presence of rat monoclonal antibody 9EG7, we used monoclonal anti-rabbit IgG antibody RG-16 coupled to alkaline phosphatase (Sigma), diluted to 1:300 in the TBS/Mg buffer containing 1% BSA. The mAb RG-16 does not cross-react with rat immunglobulin, and thus does not interfere with the ELISA. In the absence of mAb 9EG7, either the polyclonal goat anti-rabbit IgG antibody or the mAb RG-16 gave similar results. After the wells were washed four times with the TBS/Mg buffer, ELISAs were developed by adding pNpp and the absorbance was measured at 405 nm. Values for nonspecific binding, measured in the presence of 10 mM EDTA, were subtracted from total binding to give values for the specific binding of soluble $\alpha_3\beta_1$ to the immobilized ligand. Each value was determined in duplicate or triplicate, and all ligand binding assays and titration curves were repeated at least three times in independent experiments.

RESULTS

Construction, Production, and Purification of Soluble $\alpha_3\beta_1$. To produce detergent-free, soluble $\alpha_3\beta_1$ integrin, the transmembrane domains and the cytoplasmic tails of both integrin subunits were deleted. To ensure that the ectodomains associate with each other, the truncated integrin α_3 and β_1 subunits were C-terminally extended with the leucine zipper dimerization motifs of the Fos and Jun transcription factors, respectively (Figure 1). Attempts to obtain recombinant soluble $\alpha_3\beta_1$ integrin from transfected human erythroleukemic K562 cells were unsuccessful. However, cotransfection of the *Drosophila* Schneider cell line with both pUC-hygMT-α_3-Fos and pUC-hygMT-β_1-Jun and selection with hygromycin B yielded a cell population that secreted soluble $\alpha_3\beta_1$ after induction with Cu^{2+} ions. After subcloning was carried out, a stably transfected cell clone, called JAE1.1, was derived from a single cell. As estimated by a sandwich ELISA, the concentration of soluble $\alpha_3\beta_1$ integrin in JAE1.1-conditioned medium after Cu^{2+} induction was about 0.2 μg/mL.

Classical methods (ammonium precipitation, gel filtration, and ion-exchange chromatography) did not yield a pure preparation of soluble $\alpha_3\beta_1$ integrin. From Cu^{2+}-induced JAE1.1-conditioned medium, soluble $\alpha_3\beta_1$ could be purified by using affinity chromatography with anti-α_3 mAb A3-IIF5 coupled to Sepharose (data not shown). However, a requirement for harsh elution conditions (2 M urea in 1 M acetic

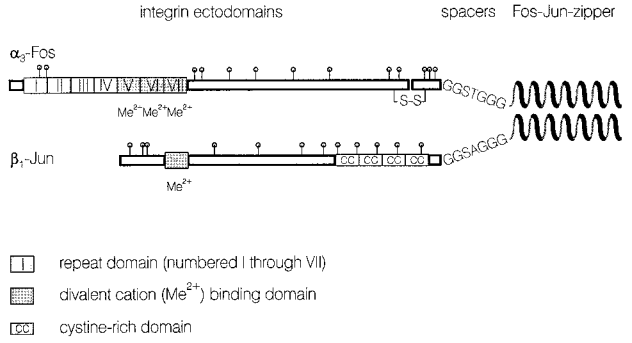

FIGURE 1: Domain structure of soluble $\alpha_3\beta_1$ integrin. The mature α_3-Fos subunit contains 1006 amino acids, not including the 32-amino acid signal sequence. The ectodomain of α_3-Fos contains repeat domains I−VII, the last three of which bind divalent cations. The α_3-Fos chain is cleaved C-terminally to a tetrabasic Arg motif. The resulting N-terminal heavy chain and the C-terminal light chain are held together by a disulfide bridge. The mature β_1-Jun subunit contains 755 amino acids after cleavage of a 20-amino acid signal sequence. The ectodomain of β_1-Jun also contains a divalent cation binding motif and four repetitive cystine-rich regions. The amino acid sequences of the heptapeptide spacers are designated for both subunits. The Fos and Jun dimerization motifs are depicted as helical structures. Potential N-glycosylation sites are indicated with lollipops.

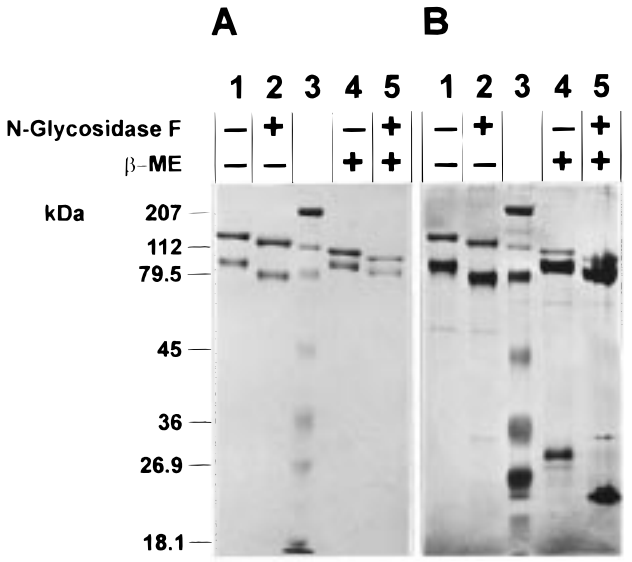

FIGURE 2: *N*-Glycosidase F digestion of soluble $\alpha_3\beta_1$ integrin. Samples of soluble $\alpha_3\beta_1$ (3 μg) were digested, as indicated, with or without *N*-glycosidase F, and separated by SDS−PAGE with or without 5% β-mercaptoethanol (βME) in the sample buffer. Samples were visualized with Coomassie blue (A) or silver (B). Lane 3 contains standard proteins with their molecular masses indicated on the left side of the gel [broad range molecular mass marker protein standard (Bio-Rad)].

acid) caused a loss of $\alpha_3\beta_1$ integrin ligand binding function. Therefore, we utilized invasin−Sepharose affinity chromatography to purify functional soluble $\alpha_3\beta_1$ under nondenaturing conditions. Binding of $\alpha_3\beta_1$ to the invasin column was assisted by the presence of 1 mM $MnCl_2$. Elution of the invasin column with 20 mM EDTA in TBS (pH 7.4) yielded pure soluble $\alpha_3\beta_1$ integrin, as shown by Coomassie- and silver-stained SDS−PAGE (Figure 2A, lanes 1 and 4; Figure 2B, lanes 1 and 4).

Under nonreducing conditions, the apparent sizes of the two integrin subunits α_3-Fos and β_1-Jun were 134 and 101 kDa, respectively (Figure 2A, lane 1; Figure 2B, lane 1).

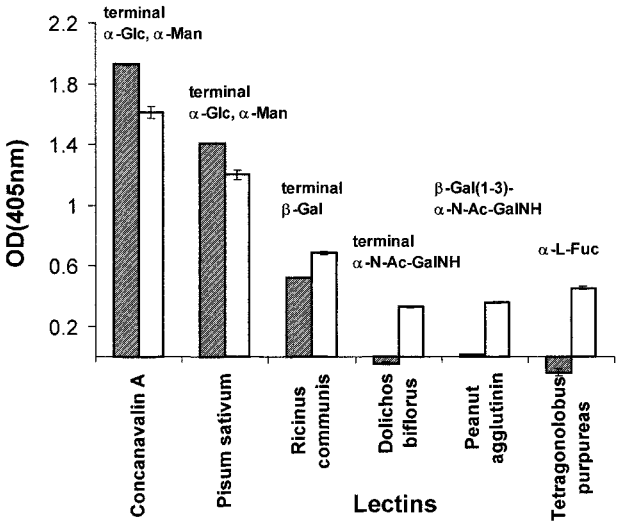

FIGURE 3: Glycoconjugate analysis of soluble human $\alpha_3\beta_1$ integrin. Immobilized $\alpha_3\beta_1$ integrin was tested with various biotinylated lectins, with each sugar binding specificity indicated. The immobilized monoclonal antibody A3-IIF5, bearing both O- and N-linked glycoconjugates, was utilized as a positive control (open bars). Assays were performed in duplicate.

Upon reduction, the α_3-Fos subunit was cleaved into heavy and light chains of 121 and 32 kDa, respectively (Figure 2A, lane 4; Figure 2B, lane 4), while the size of the β_1-Jun subunit increased to 111 kDa. Thus, the α_3-Fos and β_1-Jun subunits display electrophoretic mobilities characteristic of wild-type $\alpha_3\beta_1$. Whereas the α_3-Fos light chain is easily visualized by silver staining (Figure 2B, lane 4), it was barely stained with Coomassie (Figure 2A, lane 4).

The identity of both protein bands was confirmed in several ways. By using Western blotting, an anti-Fos polyclonal antiserum recognized the nonreduced 134 kDa α_3-Fos band, and the reduced 32 kDa α_3-Fos light chain, whereas polyclonal rabbit anti-human β_1 integrin antiserum detected the β_1-Jun chain (data not shown). Also, N-terminal sequencing of the α_3 heavy chain yielded "FNLDTR-FLVVK", thus proving that the human α_3 signal sequence was correctly cleaved by the insect cells. The α_3-Fos was always completely cleaved into heavy and light chains, but the N terminus of the α_3-Fos light chain was blocked. However, after digestion of the α_3-Fos light chain with endoproteinase Lys-C and separation of the proteolytic fragments by HPLC, the N-terminal fragment of the digested α_3-Fos light chain was identified by mass spectroscopy. To confirm its identity, this N-terminal proteolytic fragment of the α_3-Fos light chain was deblocked with pyroglutamate aminopeptidase and sequenced by Edman degradation. The sequence "(pyrGlutamate)-LDPGGGQ" shows that cleavage occurs before position 835 of the mature α_3-Fos chain. No N-terminal sequence was obtained from the β_1-Jun chain, consistent with previous evidence for a blocked N terminus (*38*). Together, these results suggest that the proteolytic processing of human soluble $\alpha_3\beta_1$ integrin in the insect cell expression system is similar to the cleavage pattern in mammalian cells.

The glycosylation pattern of our soluble human $\alpha_3\beta_1$ was first examined with lectin binding assays. As shown in Figure 3 (filled bars), soluble $\alpha_3\beta_1$ integrin was recognized by lectins (concanavalin A and *Pisum sativum* lectin) which

both bind to terminal α-mannosyl and α-glucosyl residues, indicating that the $\alpha_3\beta_1$ integrin contains mostly mannose-rich N-linked carbohydrate chains. To a lesser extent, binding of *Ricinus communis* lectin RCA_{120} demonstrated the presence of terminal β-D-galactosyl groups. These β-D-galactosyl groups typically form the nonreducing ends of both complex-type N-linked carbohydrate chains and some O-linked carbohydrate chains. However, other sugar residues typical of O-linked carbohydrates, such as the *N*-acetyl-α-D-galactosaminyl group and the β-D-galactosyl(1→3)*N*-acetyl-D-galactosaminyl disaccharide, detected by *Dolichos biflorus* and peanut agglutin lectin, respectively, were not present on the integrin. Likewise, the recombinant integrin did not bear α-L-fucosyl groups as evidenced by the lack of binding to *Tetragonolobus purpureas* lectin. α-L-Fucosyl groups are abundant in O-linked and complex-type N-linked sugar structures. Since antibodies usually bear both N- and O-linked glycoconjugates, immobilized mAb A3-IIF5 was utilized as a positive control to confirm that the lectins were functional (Figure 3, open bars).

Because the soluble $\alpha_3\beta_1$ integrin lacked α-L-fucosyl groups, N-linked carbohydrate chains should be readily susceptible to cleavage by *N*-glycosidase F. Indeed, digestion of the soluble $\alpha_3\beta_1$ integrin with *N*-glycosidase F decreased the sizes of α_3-Fos heavy, α_3-Fos light, and β_1-Jun chains by 5 (121 → 116 kDa), 7 (32 → 25 kDa), and 6 kDa (111 → 105 kDa), respectively (Figure 2A,B, lanes 2 and 5, respectively). If we assume there is 2.3 kDa per N-linked carbohydrate branch of the high mannose type, only two or three of the 12 potential N-linked glycosylation sites (Figure 1) may be occupied in the β_1 ectodomain, and only two of 10 may be present in the α_3-Fos heavy chain. However, three of three potential N-glycosylation sites appear to be occupied in the α_3-Fos light chain.

Ligand Binding Specificity of the Soluble $\alpha_3\beta_1$ Integrin. Various extracellular matrix proteins have been proposed to be ligands for the $\alpha_3\beta_1$ integrin, often on the basis of cell adhesion studies (see the introductory section). Here, with the availability of highly purified soluble $\alpha_3\beta_1$, direct protein−protein binding studies were made feasible. As indicated in Figure 4 (filled bars), purified soluble $\alpha_3\beta_1$ bound strongly to laminin-5, and placental laminin (mostly laminin-10), and to a much lesser extent to laminin-2. No binding to fibronectin, to the fibrillar type I, III, and V collagens, or to thrombospondin-1 was observed. Interestingly, no basal membrane components other than laminin-5 and laminin-10, namely, collagen type IV, laminin-1, or nidogen/entactin, were recognized by the soluble $\alpha_3\beta_1$ integrin. Because complement protein C3 and its fragments appear to colocalize with $\alpha_3\beta_1$ along the basal layer of skin epidermis and kidney epithelium (*39*), we also tested the uncleaved and cleaved complement C3 and C3b proteins and did not see binding. The fusion protein MBP−invasin was used as a positive control for integrin binding activity. To optimize binding, 1 mM Mn^{2+} was included in the assays. There was minimal nonspecific integrin binding to any putative ligand, as determined in the presence of 10 mM EDTA (Figure 4, open bars).

Titration of Immobilized Laminin-5 and Invasin with Soluble $\alpha_3\beta_1$ Integrin. To better assess the interaction of soluble $\alpha_3\beta_1$ integrin with laminin-5 and invasin, integrin titrations were carried out in 1 mM Mn^{2+}. Coating concentrations of 5 μg/mL laminin-5 and 4 μg/mL MBP−invasin were sufficient to give a strong ELISA signal for bound integrin. As shown in Figure 5A, specific binding of soluble $\alpha_3\beta_1$ to immobilized laminin-5 (solid line) could be determined from total binding (upper dashed line) minus nonspecific binding, determined in the presence of 10 mM EDTA (lower dashed line). In Figure 5B, total and specific $\alpha_3\beta_1$ binding to invasin were essentially identical, since there was minimal nonspecific binding (lower dashed line). The specific binding of soluble $\alpha_3\beta_1$ to both laminin-5 and MBP−invasin reaches saturation, albeit at different concentrations of the integrin receptor. Semilogarithmic plots of specific $\alpha_3\beta_1$ binding (Figure 5C) indicate that the affinity of $\alpha_3\beta_1$ integrin for invasin is approximately 100-fold higher than its affinity for laminin-5. Using the algorithm of Heyn and Weischet (*40*), $\alpha_3\beta_1$ bound to MBP−invasin with a K_d of 0.29 ± 0.05 nM, whereas the K_d for laminin-5 was 27 ± 7 nM.

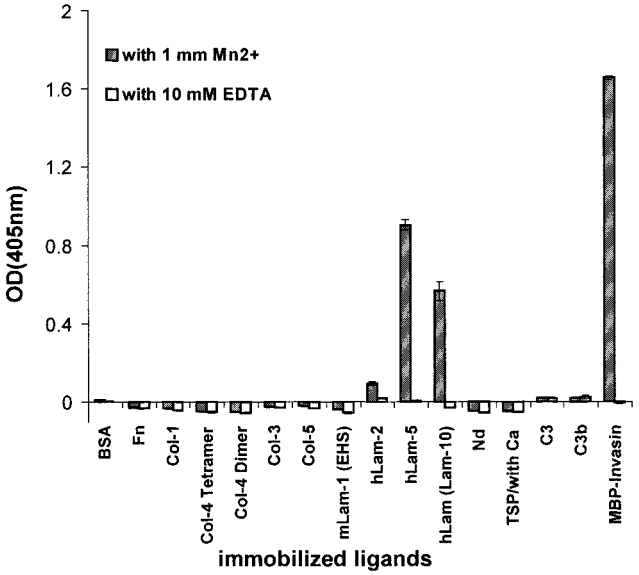

FIGURE 4: Ligand binding specificity of soluble $\alpha_3\beta_1$ integrin. Purified ligands (Fn = fibronectin, Col = collagen, mLam = mouse laminin, hLam = human laminin, Nd = nidogen, and TSP = thrombospondin) were coated at 20 μg/mL, except for MBP−invasin, which was applied at 4 μg/mL to the microtiter plate. Soluble $\alpha_3\beta_1$ (100 nM) integrin was allowed to bind to the immobilized ligands in the presence of either divalent cations (2 mM $MgCl_2$ and 1 mM $MnCl_2$) or 10 mM EDTA, indicated by shaded and white bars, respectively. The latter condition measures nonspecific binding. After washing and fixation, the amount of bound $\alpha_3\beta_1$ integrin was quantified with an ELISA, as described in Experimental Procedures. The averages of triplicate determinations are shown. Error bars represent standard deviations. The entire assay was repeated several times with the same results as shown here.

In further studies, we determined the regulation of $\alpha_3\beta_1$ integrin binding by divalent cations and by an activating anti-β_1 mAb. Under basal conditions [TBS (pH 7.2) with 2 mM $MgCl_2$], $\alpha_3\beta_1$ again bound with much greater apparent affinity for invasin (Figure 6, open triangles) than for laminin-5 (closed triangles) as seen in semilogarithmic plots. When 1 mM Mn^{2+} was added, the titration curves for both ligands were shifted by about 10-fold to the left (compare open and closed circles relative to open and closed triangles in Figure 6). Similarly, the apparent affinity for invasin and laminin-5 was increased upon addition of anti-β_1 activating

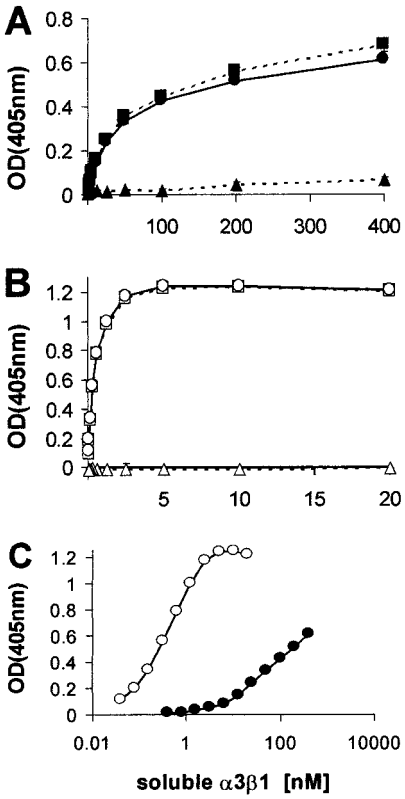

FIGURE 5: Titration of immobilized laminin-5 and MBP−invasin with soluble $\alpha_3\beta_1$. Laminin-5 (A) and MBP−invasin (B) were immobilized on microtiter plates at 5 and 4 μg/mL, respectively. After blocking nonspecific binding sites, soluble $\alpha_3\beta_1$ integrin was allowed to bind in the presence of either divalent cations (2 mM $MgCl_2$ and 1 mM $MnCl_2$) or 10 mM EDTA, symbolized by dotted lines with squares and triangles, respectively. After washing and fixation, the bound integrin receptor was determined with an ELISA as described. Specific binding of the integrin to its respective ligand (circles and straight line) was calculated as the difference between total binding, measured in the presence of divalent cations (symbolized by squares and a dotted line), and nonspecific binding (symbolized by triangles and a dotted line), observed in the presence of 10 mM EDTA. The titration curves for specific binding were linearized according to Heyn and Weischet, and K_d values were determined. (C) Titration curves for specific $\alpha_3\beta_1$ binding to laminin (black symbols) and MBP−invasin (white symbols) were combined in a semilogarithmic plot.

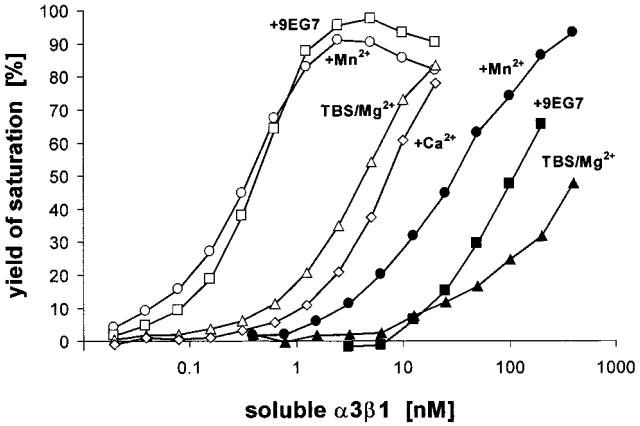

FIGURE 6: Regulation of $\alpha_3\beta_1$ binding to laminin-5 and MBP−invasin. Laminin-5 (black symbols) and MBP−invasin (white symbols) were immobilized at 5 and 4 μg/mL, respectively. After blocking of nonspecific binding sites, $\alpha_3\beta_1$ was allowed to bind either in standard TBS buffer containing 2 mM $MgCl_2$ (triangles) or after addition of 1 mM $MnCl_2$ (circles), monoclonal antibody 9EG7 (squares), or 2 mM $CaCl_2$ (diamonds). Monoclonal antibody 9EG7 (at >6 μg/mL) was always in an at least 2-fold molar surplus with respect to the soluble integrin. Nonspecific binding was measured in the presence of 10 mM EDTA and is subtracted. All binding was determined in duplicate. Only specific binding curves are shown, and the values are normalized to the maximal binding value to give the yield of saturation. Maximal binding of laminin-5 and MBP−invasin corresponds to specific OD(405 nm) values of 0.34 and 0.8, respectively.

Table 1: K_d Values for $\alpha_3\beta_1$ Binding to Laminin-5 and MBP−Invasin[a]

conditions	K_d for binding to laminin-5 (nM)	K_d for binding to MBP−invasin (nM)
with 1 mM Mn^{2+}	27 ± 7 (n = 4)	0.29 ± 0.05 (n = 5)
with mAb 9EG7	88 (n = 1)	0.1 (n = 1)
without additives (TBS and 2 mM Mg^{2+})	>600 (n = 3)	3.1 ± 1.2 (n = 3)
with 2 mM Ca^{2+}	nd	5.4 ± 2.0 (n = 3)

[a] Binding was determined in the TBS buffer (pH 7.4) containing 2 mM $MgCl_2$, with or without further addition of 1 mM Mn^{2+}, or monoclonal anti-integrin β_1-antibody 9EG7, or 2 mM Ca^{2+}. The number of titration curves used for the evaluation is indicated in parentheses. nd means not determined.

mAb 9EG7 (see open and closed squares), whereas the affinity for invasin was decreased upon addition of 2 mM Ca^{2+} (open diamonds). We expect that Ca^{2+} should also decrease the affinity of $\alpha_3\beta_1$ for laminin-5, but this could not be determined because (i) such low-affinity interactions are not maintained during washing steps and (ii) amounts of soluble $\alpha_3\beta_1$ required for saturation are prohibitive. Interestingly, titration curves in the presence of 9EG7 not only are shifted to lower integrin concentrations but also show a steeper slope, suggestive of allosteric effects.

From titration curves such as those in Figure 6, K_d values were calculated, and they are summarized in Table 1. Whereas $\alpha_3\beta_1$ binding to laminin-5 under nonactivating conditions had a comparatively low affinity (K_d > 600 nM), affinity for laminin-5 was increased by more than 20-fold by 1 mM Mn^{2+} (to 27 nM) and by more than 7-fold by 9EG7 (to 88 nM). For binding to invasin, the basal binding activity (K_d = 3.1 nM) was increased by 10−30-fold upon the addition of Mn^{2+} and 9EG7, to yield affinites of 0.29 and 0.1 nM, respectively. Conversely, the affinity for invasin was decreased nearly 2-fold to 5.4 nM upon addition of Ca^{2+} ions. As seen in an inhibition assay (Figure 7), soluble MBP−invasin could completely inhibit the binding of soluble $\alpha_3\beta_1$ to immobilized laminin-5. Because of the poor solubility of laminin-5, the reciprocal inhibition test could not be performed. Nevertheless, the complete inhibition of the $\alpha_3\beta_1$−laminin-5 interaction by MBP−invasin suggests that the two ligands bind to sites on the $\alpha_3\beta_1$ integrin that are close together or even identical.

DISCUSSION

Here we describe the first preparation of recombinant soluble $\alpha_3\beta_1$ integrin. Soluble human $\alpha_3\beta_1$ integrin, containing a Fos−Jun zipper, has been purified in high yield. This soluble integrin has allowed us, for the first time, to estimate ligand binding constants for $\alpha_3\beta_1$. Thus, we have learned that (i) $\alpha_3\beta_1$ bound >100-fold better to the bacterial invasin protein than to laminin-5, its endogenous ligand, (ii) Mn^{2+} markedly stimulated $\alpha_3\beta_1$ ligand binding, even though

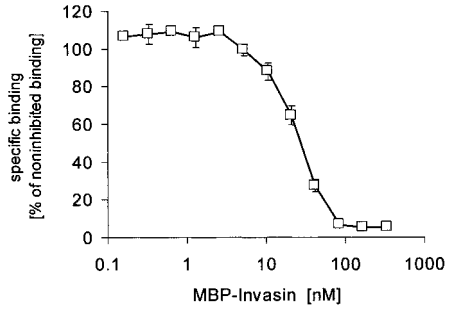

FIGURE 7: Binding of $\alpha_3\beta_1$ integrin to immobilzed laminin-5 is inhibited by soluble MBP−invasin. Laminin-5 was coated onto the microtiter plate at 5 μg/mL. After nonspecific binding sites had been blocked, soluble $\alpha_3\beta_1$ integrin (at 60 nM) was added in the presence of the indicated concentration of soluble MBP−invasin. After the wells were washed four times with 25 mM HEPES buffer (pH 7.6) containing 2 mM $MgCl_2$ and 1 mM $MnCl_2$, bound integrin was fixed for 10 min with 2.5% glutaraldehyde in the same solution. After three washes with the TBS/Mg buffer, the amount of $\alpha_3\beta_1$ bound to the immobilized laminin-5 was measured with an ELISA. The wells were subsequently incubated with anti-human β_1-antiserum and the anti-rabbit IgG antibody−alkaline phosphatase conjugate, each diluted in the TBS/Mg buffer containing 1% BSA, and followed by three washes with the TBS/Mg buffer. The ELISA was developed with *p*-nitrophenyl phosphate and the absorbance read at 405 nm. The absorbance values were corrected for the nonspecific binding, measured in the presence of 10 mM EDTA, and finally normalized to the uninhibited binding [OD(405 nm) = 0.49], measured in the absence of soluble MBP−invasin. The assay was performed in duplicate.

previous studies showed that Mn^{2+} failed to induce detectable new epitopes on $\alpha_3\beta_1$, and (iii) most of the suspected ligands showed no binding, even in the presence of 1 mM Mn^{2+}. In addition to gaining important insights into the specificity, affinity, and regulation of $\alpha_3\beta_1$ ligand binding, we have also determined the site at which α_3 undergoes proteolytic processing and evaluated both the type and amount of integrin glycosylation. Besides it being a useful tool for obtaining definitive functional and structural results, we also suggest that our recombinant $\alpha_3\beta_1$ may be a good starting point for attempts at integrin crystallization.

Solubilization of integrins by deletion of the cytoplasmic and transmembrane domains has so far been successful for the expression of integrin heterodimers $\alpha_L\beta_2$ (*41*) and $\alpha_{IIb}\beta_3$ (*42*−*44*), $\alpha_1\beta_1$ (*45*), $\alpha_V\beta_6$ (*46*), and $\alpha_V\beta_8$ (*47*). Nonetheless, prior studies with β_1-integrins have established that transmembrane and cytoplasmic domains may importantly contribute to the formation and stability of β_1 integrin heterodimers (*45*). Indeed, attempts to express a truncated heterodimer consisting of the integrin α_6 and β_1 ectodomains were unsuccessful (A. Sonnenberg, personal communication). Thus, rather than simply deleting transmembrane and cytoplasmic domains, we have replaced them with the Fos and Jun leucine zipper domains, and have produced a stable $\alpha_3\beta_1$ heterodimer. Although previous studies have shown that deletion of integrin cytoplasmic domains can alter integrin function in the cellular context (*48*), there was no reason to expect that their absence would affect ligand binding affinity and specificity in a cell-free system. Furthermore, in our system, the α helical structures of both transmembrane domains are replaced by structurally similar, amphipathic α helices of the Fos and Jun protein, respectively. With this strategy, we hoped to better maintain the structure of the soluble $\alpha_3\beta_1$ integrin ectodomains. Indeed, our recombinant $\alpha_3\beta_1$ shows specificity of ligand binding and affinity for laminin-5 that is comparable to affinities of other integrins for their ECM ligands (*49*−*51*). The affinity of our soluble $\alpha_3\beta_1$ for invasin is also comparable to the affinity of wild-type $\alpha_5\beta_1$ for invasin (*52*).

Previously, expression of soluble integrins in mammalian cell lines often yielded only small amounts, as detected by metabolic labeling or by radioimmunoassay (*41*, *43*, *45*, *53*). In one study, Dana et al. (*49*) prepared soluble $\alpha_M\beta_2$ integrin at 20 μg/L. Although binding activity was demonstrated in these reports, integrin quantities were too low to allow determination of ligand binding affinities. Here we have prepared large quantities of recombinant soluble $\alpha_3\beta_1$ (up to 250 μg per liter). Our high yield of recombinant $\alpha_3\beta_1$ may result partly from the use of the Schneider insect cell line and the inducible metallothionin promoter to produce α_3-Fos and β_1-Jun. We did not observe synthesis of soluble $\alpha_3\beta_1$ integrin in the mammalian cell line K562, under the constitutively active SV40 promoter. One posibility is that, compared to the growth of mammalian cells at 37 °C, the growth of insect cells at 25 °C may allow the proper folding and assembly of the two integrin subunits.

Another reason for high yields of recombinant $\alpha_3\beta_1$ appears to be the use of the Fos−Jun leucine zipper motifs to promote stable subunit association. These α helical dimerization motifs, each consisting of approximately 40 residues with the characteristic leucine zipper heptad repeats, spontaneously associate into a coiled-coil structure because of hydrophobic interactions. The outer faces of the amphipolar α helices contain hydrophilic and charged residues and make the coiled-coil structure fully water-soluble (*54*). Thus, the Fos and Jun motif allows integrin ectodomains to dimerize and to stay in solution without detergent. Dimerizing leucine zipper motifs have already been used successfully to greatly facilitate the production of bispecific F_{ab}-heterodimers (*55*) and soluble T cell receptor (*56*) and MHC class II (*57*) heterodimers. For example, the dimerizing motif of Fos and Jun increases the efficiency of T cell receptor production by 5−10-fold (*56*) and allows the expression of HLA-DR (*57*). Our system produces about 10 times the amount of soluble $\alpha_3\beta_1$, compared to the amount of soluble $\alpha_1\beta_2$ integrin prepared by Dana et al. (*49*). Besides other factors, we think that the use of the Fos−Jun dimerization motif is partially responsible for this increase in production efficiency. Since the dimerizing motif of Fos (*54*) and the integrin β ectodomain (*44*, *53*) are by themselves prone to homodimerization, the Fos-dimerizing motif was fused to the α_3 ectodomain and the Jun-dimerizing motif was added to the β_1 ectodomain. Unlike in other studies expressing soluble integrin ectodomains (*42*, *43*), we saw no evidence of homodimerization. After immunodepletion of crude insect cell supernatant three times with anti-α_3 antibody, we could not then precipitate any unassociated β_1-Jun. Conversely, after immunodepletion three times with anti-β_1 antibody, we could not then precipitate any unassociated α_3-Fos. Furthermore, all immunoprecipitated material contained α_3-Fos and β_1-Jun in equimolar amounts with no evidence of immature, unprocessed precursors. Thus, the JAE1.1 cells appear to secrete only mature α_3-Fos and β_1-Jun subunits which are exclusively associated stoichiometrically into a 1:1 heterodimeric complex.

Using invasin−Sepharose affinity chromatography, we obtained a high yield of fully functional recombinant $\alpha_3\beta_1$. Advantages of invasin−Sepharose purfication are several. First, the high affinity of invasin for $\alpha_3\beta_1$ (K_d < 1 nM in the presence of Mn^{2+}) allows for efficient capture of soluble integrins. Second, elution with EDTA easily releases the integrin while maintaining its native conformation. Finally, use of invasin−Sepharose selects exclusively for fully functional integrin heterodimers. In contrast, immunopurification on beads coated with anti-α_3 integrin mAbs requires elution under conditions that are at least partially denaturing and usually result in contamination of the integrin preparation with the mAb.

Perhaps the most important evidence for the structural authenticity of our recombinant $\alpha_3\beta_1$ protein is that (i) it bound to ligands with a high degree of specificity and reasonable affinity and (ii) its ligand binding function was regulated by activating and attenuating reagents, e.g., Mn^{2+}, activating mAb, and Ca^{2+}, respectively, as has been seen for wild-type $\alpha_3\beta_1$ (see below). In addition, we determined that the α chain signal sequence was correctly removed and the α_3-Fos subunit, like the wild-type α_3 subunit in mammalian cells, was proteolytically cleaved into disulfide-linked heavy and light chains. Importantly, proteolytic processing of α_3 (just after a tetrabasic motif) within our secreted recombinant soluble $\alpha_3\beta_1$ exactly corresponds to the site of cleavage in α_6 in mammalian cells (*58*). A similar site is also utilized in mammalian cells for cleavage of α_7, α_{IIb}, and other endoproteolytically cleaved integrin α subunits. The information provided here now makes it feasible to prepare α_3 mutants, which should be useful in proving that the identical endoproteolytic cleavage site is used in human cells, and in functional studies such as those carried out for the integrin α_6 subunit lacking this endoproteolytic cleavage (*58*).

It is unlikely that glycosylation occurring in insect cells would be identical to that seen in mammalian cells. Nonetheless, decreases in size upon deglycosylation of the recombinant α_3 and β_1 subunits using *N*-glycosidase F are comparable to decreases in size seen for mammalian $\alpha_3\beta_1$ and $\alpha_6\beta_1$ integrins (*59*). The human soluble $\alpha_3\beta_1$ integrin expressed by Schneider insect cells does not contain common O-linked glycosylation structures, and thus, the binding of RCA_{120} lectin to $\alpha_3\beta_1$ integrin is likely explained by terminal β-galactosyl groups attached to complex-type N-linked carbohydrate side chains. The lack of α-L-fucosyl groups, which are found in N-linked glycoconjugates of the complex type, and the comparatively low level of RCA_{120} binding suggest that insect cells largely fail to process the N-attached glycoconjugates into complex-type structures, but rather maintain most of the N-linked carbohydrate side chains in the high-mannose form. Furthermore, only a fraction of the possible N-glycosylation sites within the α_3 heavy chain and the β_1 subunit appeared to be occupied. However, the integrin α_3-Fos light chain bore N-linked glycoconjugates on all three of its potential N-glycosylation sites. We hypothesize that the bulky carbohydrate side chains may stabilize the elongated stalk structure of the C-terminal portion of the integrin ectodomain and protect it from proteolytic degradation.

Preparation of recombinant soluble $\alpha_3\beta_1$ integrin, as described here, allowed definitive analysis of ligand binding specificity. The purified $\alpha_3\beta_1$ integrin is a very specific receptor for particular isoforms of laminin. The integrin did not recognize mouse laminin-1 ($\alpha1\beta1\gamma1$), minimally recognized human laminin-2 ($\alpha2\beta1\gamma1$), and substantially recognized placental laminin, which mainly consists of laminin-10 ($\alpha5\beta1\gamma1$) (*34*, *35*). Considering (i) that mouse laminin-1, human laminin-2, and human laminin-10 differ in their α chains and (ii) that mouse and human laminin chains have a high degree of sequence homolgy (*60*), we assume that the laminin α chain determines the specificity for recognition by the $\alpha_3\beta_1$ integrin. Laminin-5 ($\alpha3\beta3\gamma2$) is the isoform bound most avidly by the $\alpha_3\beta_1$ integrin. We surmise that the α3 chain of laminin-5 accounts for the specific and high-affinity interaction with the soluble $\alpha_3\beta_1$ receptor. The α3 chain of laminin-5 is highly similar to the α5 chain of laminin-10 (*61*), which is recognized by $\alpha_3\beta_1$ integrin as well. However, since all three chains of the laminin molecule are necessary to maintain the molecular conformation, we cannot exclude the possibility that the laminin β and γ chains influence the $\alpha_3\beta_1$−laminin interaction.

Our results are consistent with cell adhesion studies previously demonstrating that integrin $\alpha_3\beta_1$ is involved in cell attachment to laminin-5 (*16*, *17*, *26*). Furthermore, $\alpha_3\beta_1$-bearing cells often colocalize with laminin-5 containing basal membranes in tissue (*11*). Both laminin-5 and laminin-10 are abundant in basement membranes of epithelial tissue and share a similar tissue distribution in kidney and lung (*35*), organs strongly affected by the integrin α_3 knockout (*8*). The interaction of $\alpha_3\beta_1$ integrin with laminin-5 plays a crucial role on keratinocytes of the basal layer of the epidermis (*7*). As the main constituent of the anchoring filaments in the *lamina lucida* of the basal membrane, laminin-5 is close to the keratinocyte cell surface. No other component of the basal membrane bound to soluble $\alpha_3\beta_1$ integrin. Lacking $\alpha_3\beta_1$ integrin, keratinocytes of α_3 knockout mice lose their contacts with the basal membrane and the whole cell layer detaches as a blister (*9*).

Several extracellular matrix proteins, including fibronectin, collagen, laminin-1 (*14*), nidogen/entactin (*18*), and thrombospondin (*19*), have previously been suggested to be ligands for the $\alpha_3\beta_1$ integrin, but were not recognized by our recombinant soluble $\alpha_3\beta_1$. Here we show no detectable interaction of soluble $\alpha_3\beta_1$ with any of these ligands, even in the presence of 1 mM Mn^{2+}. Our studies do not necessarily contradict prior $\alpha_3\beta_1$ cell adhesion studies, but rather shed light on the direct and primary interaction of purified, detergent-free $\alpha_3\beta_1$ with its various proposed ligands, which eventually mediates $\alpha_3\beta_1$-dependent cell adhesion. One possibility is that $\alpha_3\beta_1$ interactions with some ligands may be sufficiently avid to support cell adhesion, even though they do not have sufficient affinity to be measured as positive in our ligand binding assay. For example, we may have missed weak ligand interactions in Figure 4 if the K_d was higher than 10 μM. Alternatively, blocking of cell adhesion by anti-α_3 antibodies could occur because $\alpha_3\beta_1$ behaves as an indirect secondary receptor with post-cell adhesion functions, which is recruited into focal contacts of cells plated on extracellular matrix proteins that are not recognized by the $\alpha_3\beta_1$ integrin itself (*62*). In addition, prior ligand binding assays using detergent-solubilized $\alpha_3\beta_1$ may have been complicated by the presence of multivalent detergent micelles, and by the apparent capability

of $\alpha_3\beta_1$ to associate with several other transmembrane proteins (*63*, *64*). On the other hand, the lack of membrane or micelle components or the substitution of the transmembrane and cytoplasmic tails of both subunits by the Fos−Jun dimerizing motif in our soluble $\alpha_3\beta_1$ integrin may affect ligand binding in our test system. Different glycoconjugate processing of the soluble $\alpha_3\beta_1$ integrin in the insect cells may also account for discrepancies in ligand binding specificities, although we could not see any altered binding to laminin-5 and invasin of soluble $\alpha_3\beta_1$ integrin after complete shedding of the N-linked carbohydrate chains by *N*-glycosidase F treatment.

In the presence of 2 mM Mg^{2+}, soluble $\alpha_3\beta_1$ integrin had a comparatively low binding affinity of >600 nM for laminin-5 (Table 1), and the affinity was even lower if Ca^{2+} was present, reflecting conditions that are found in the serum and tissue. Thus $\alpha_3\beta_1$, like other integrins, engages in relatively low-affinity interactions with ECM proteins, which would perhaps allow a migratory role of the $\alpha_3\beta_1$ integrin, as was proposed for re-epithelization during wound healing (*7*). In the presence of 1 mM Mn^{2+}, the $\alpha_3\beta_1$ affinity for both laminin-5 and invasin increased markedly, although the affinity for laminin-5 still remained much weaker than the affinity for invasin. These results are consistent with the general capability of Mn^{2+} to stimulate integrin affinity for ligands (*15*, *65*−*67*). Elsewhere, we found that Mn^{2+} induces the appearance of new epitopes, as defined by mAbs 9EG7 and 15/7, on other integrins (e.g., $\alpha_4\beta_1$ and $\alpha_5\beta_1$) but not on membrane-anchored wild-type mammalian $\alpha_3\beta_1$ (*68*). Similarly, titration of soluble $\alpha_3\beta_1$ with Mn^{2+} ion up to 16 mM did not increase the presentation of the 9EG7 epitope. Nonetheless, we show here that Mn^{2+} does greatly stimulate $\alpha_3\beta_1$ ligand binding. Thus, for both wild-type and recombinant $\alpha_3\beta_1$, Mn^{2+} effects on ligand binding can be clearly dissociated from Mn^{2+} induction of neoepitopes.

The affinity for both laminin-5 and invasin was also significantly stimulated by the anti-β_1 activating antibody 9EG7. Results obtained here (laminin-5, $K_d \approx 88$ nM, in the presence of 9EG7) are in the range of those K_d values (9, 18, and ≈800 nM) obtained for activating antibody-stimulated fibronectin binding to $\alpha_5\beta_1$ (*50*), laminin binding to $\alpha_2\beta_1$ (*69*), and VCAM-1 binding to $\alpha_4\beta_1$ (*70*). For 9EG7-stimulated binding, the steeper titration curve in the semilogarithmic plot suggests that 9EG7 may function as an allosteric effector, by helping the ligand induce a conformational change toward a higher-affinity state of the integrin receptor, as discussed for the $\alpha_5\beta_1$ integrin (*67*). Thus, the activation of the soluble $\alpha_3\beta_1$ integrin could be interpreted as an alteration of the integrin conformation. However, structural studies will have to corroborate this hypothesis.

Of special interest is the nearly 100-fold higher affinity of $\alpha_3\beta_1$ for invasin, compared to that for laminin-5. This result mimics the substantially greater affinity of the $\alpha_5\beta_1$ integrin for invasin, compared to that for fibronectin (*52*). These results, together with the finding that soluble invasin can completely inhibit $\alpha_3\beta_1$ binding to laminin-5, support the idea that invasin-bearing species of *Yersinia* may readily subvert normal integrin-dependent epithelial cell adhesion to extracellular matrix proteins so that integrins instead support bacterial uptake (*20*). Potentially, soluble $\alpha_3\beta_1$ integrin could be a useful tool for treating those bacterial infections caused by the invasin-bearing species of *Yersinia*.

In summary, we have prepared large amounts of recombinant soluble $\alpha_3\beta_1$ integrin that is endoproteolytically processed, fully functional, and appropriately regulated. With this detergent-free preparation, we determined that $\alpha_3\beta_1$ is a highly specific receptor and has a reasonable affinity for laminin-5 and laminin-10, and an even greater affinity for the pathogenic ligand invasin. Our recombinant $\alpha_3\beta_1$ preparation not only has provided important functional insights but also could be a useful starting point for integrin crystallization.

ACKNOWLEDGMENT

We thank James F. Lee for assistance in protein sequencing. The support and interest given to this work by Prof. K. Kühn, Dr. R. Timpl, and Dr. Brian A. Mannion is also gratefully acknowledged.

REFERENCES

1. Eble, J. A. (1997) in *Integrin-ligand interaction* (Eble, J. A., and Kühn, K., Eds.) pp 3−40, R. G. Landes, Austin, TX, and Springer, Heidelberg, Germany.
2. Hynes, R. O. (1992) *Cell 69*, 11−25.
3. Nermut, M. V., Green, N. M., Eason, P., Yamada, S. S., and Yamada, K. M. (1988) *EMBO J. 7*, 4093−4099.
4. Sastry, S. K., and Horwitz, A. F. (1993) *Curr. Opin. Cell Biol. 5*, 819−831.
5. Briesewitz, R., Kern, A., and Marcantonio, E. E. (1993) *Mol. Biol. Cell 4*, 593−604.
6. Weitzman, J. B., Hemler, M. E., and Brodt, P. (1996) *Cell Adhes. Commun. 4*, 41−52.
7. Larjava, H., Salo, T., Haapasalmi, K., Kramer, R. H., and Heino J. (1993) *J. Clin. Invest. 92*, 1425−1435.
8. Kreidberg, J. A., Donovan, M. J., Goldstein, S. L., Rennke, H., Sheppard, K., Jones, R. C., and Jaenisch, R. (1996) *Development 122*, 3537−3547.
9. DiPersio, C. M., Hodivala-Dilke, K. M., Jaenisch, R., Kreidberg, J. A., and Hynes, R. O. (1997) *J. Cell Biol. 137*, 729−742.
10. Rousselle, P., Lunstrum, G. P., Keene, D. R., and Burgeson, R. E. (1991) *J. Cell Biol. 114*, 567−576.
11. Carter, W. G., Ryan, M. C., and Gahr, P. J. (1991) *Cell 65*, 599−610.
12. Timpl, R. (1996) *Curr. Opin. Cell Biol. 8*, 618−624.
13. Wayner, E. A., and Carter, W. G. (1987) *J. Cell Biol. 105*, 1873−1884.
14. Elices, M. J., Urry, L. A., and Hemler, M. E. (1991) *J. Cell Biol. 112*, 169−181.
15. Gehlsen, K. R., Dillner, L., Engvall, E., and Rouslahti, E. (1988) *Science 241*, 1228−1229.
16. Delwel, G. O., de Melker, A. A., Hogervorst, F., Jaspars, L. H., Fles, D. L. A., Kuikman, I., Lindblom, A., Paulsson, M., Timpl, R., and Sonnenberg, A. (1994) *Mol. Biol. Cell 5*, 203−215.
17. Wayner, E. A., Gil, S. G., Murphy, G. F., Wilke, M. S., and Carter, W. G. (1993) *J. Cell Biol. 121*, 1141−1152.
18. Dedhar, S., Jewell, K., Rojiani, M., and Gray V. (1992) *J. Biol. Chem. 267*, 18908−18914.
19. DeFreitas, M. F., Yoshida, C. K., Frazier, W. A., Mendrick, D. L., Kypta, R. M., and Reichardt, L. F. (1995) *Neuron 15*, 333−343.
20. Isberg, R. R., and Leong, J. M. (1990) *Cell 60*, 861−871.
21. Leong, J. M., Fournier, R. S., and Isberg, R. R. (1990) *EMBO J. 9*, 1979−1989.
22. Takada, Y., Murphy, E., Pil, P., Chen, C., Ginsberg, M. H., and Hemler, M. E. (1991) *J. Cell Biol. 115*, 257−266.
23. Rio, D. C., Laski, F. A., and Rubin, G. M. (1986) *Cell 44*, 21−32.
24. Bunch, T. A., Grinblat, Y., and Goldstein, L. S. B. (1988) *Nucleic Acids Res. 16*, 1043−1061.

25. Argraves, W. S., Suzuki, S., Arai, H., Thompson, K., Pierschbacher, M. D., and Ruoslahti, E. (1987) *J. Cell Biol. 105*, 1183−1190.
26. Weitzman, J. B., Pasqualini, R., Takada, Y., and Hemler, M. E. (1993) *J. Biol. Chem. 268*, 8651−8657.
27. Eble, J. A. (1994) Die dreidimensionale Struktur der Erkennungsregion des $\alpha_1\beta_1$-Integrins im Typ IV-Kollagen, Thesis LMU München, pp 37−38, Verlag Shaker Aachen.
28. Strauch, K. L., and Beckwith, J. (1988) *Proc. Natl. Acad. Sci. U.S.A. 85*, 1576−1580.
29. Rousselle, P., and Aumailley M. (1994) *J. Cell Biol. 125*, 205−214.
30. Marinkovich, M. P., Lunstrum, G. P., and Burgeson, R. E. (1992) *J. Biol. Chem. 267*, 17900−17906.
31. Timpl, R., Wiedemann, H., Van Delden, V., Furthmayr, H., and Kühn, K. (1981) *Eur. J. Biochem. 120*, 203−211.
32. Kühn, K. (1994) *Matrix Biol. 14*, 439−445.
33. Fox, J. W., Mayer, U., Nischt, R., Aumailley, M., Reinhardt, D., Wiedemann, H., Mann, K., Timpl, R., Krieg, T., Engel, J., and Chu, M.-L. (1991) *EMBO J. 10*, 3137−3146.
34. Tiger, C. F., Champliaud, M.-F., Pedrosa-Domellof, F., Thornell, L. E., Ekblom, P., and Gullberg, D. (1997) *J. Biol. Chem. 272*, 28590−28595.
35. Miner, J. H., Patton, B. L., Lentz, S. I., Gilbert, D. J., Snider, W. D., Jenkins, N. A., Copeland, N. G., and Sanes, J. R. (1997) *J. Cell Biol. 137*, 685−701.
36. Lenter, M., Uhlig, H., Hamann, A., Jenö, P., Imhof, B., and Vestweber, D. (1993) *Proc. Natl. Acad. Sci. U.S.A. 90*, 9051−9055.
37. Bazzoni, G., Shih, D.-T., Buck, C. A., and Hemler, M. E. (1995) *J. Biol. Chem. 270*, 25570−25577.
38. Takada, Y., Strominger, J. L., and Hemler, M. E. (1987) *Proc. Natl. Acad. Sci. U.S.A. 84*, 3239−3243.
39. Yancey, K. B., and Basset-Sequin, N. (1990) *J. Invest. Dermatol. 94*, 122s−127s.
40. Heyn, M. P., and Weischet W. O. (1975) *J. Biol. Chem. 242*, 2962−2968.
41. Dana, N., Fathallah, D. M., and Arnout, M. A. (1991) *Proc. Natl. Acad. Sci. U.S.A. 88*, 3106−3110.
42. Wippler, J., Kouns, W. C., Schalaeger, E.-J., Kuhn, H., Hadvary, P., and Steiner, B. (1994) *J. Biol. Chem. 269*, 8754−8761.
43. Gulino, D., Martinez, P., Delachanal, E., Concord, E., Duperray, A., Alemany, M., and Marguerie, G. (1995) *Eur. J. Biochem. 227*, 108−115.
44. McKay, B. S., Annis, D. S., Honda, S., Christie, D., and Kunicki, T. J. (1996) *J. Biol. Chem. 271*, 30554−30547.
45. Briesewitz, R., Epstein, M. R., and Marcantonio, E. E. (1993) *J. Biol. Chem. 268*, 2989−2996.
46. Weinacker, A., Chem, A., Agrez, M., Cone, R. I., Nishimura, S., Wayner, E., Pytela, R., and Sheppard, D. (1994) *J. Biol. Chem. 269*, 6940−6948.
47. Nishimura, S. L., Sheppard, D., and Pytela, R. (1994) *J. Biol. Chem. 269*, 28708−28715.
48. Kassner, P. D., Kawaguchi, S., and Hemler, M. E. (1994) *J. Biol. Chem. 269*, 19859−19867.
49. Kern, A., Eble, J., Golbik, R., and Kühn, K. (1993) *Eur. J. Biochem. 215*, 151−159.
50. Faull, R. J., Kovach, N. L., Harlan, J. M., and Ginsberg, M. H. (1994) *J. Exp. Med. 179*, 1307−1316.
51. Tangemann, K., and Engel, J. (1997) in *Integrin-ligand interaction* (Eble, J. A., and Kühn, K., Eds.) pp 85−100, R. G. Landes, Austin, TX, and Springer, Heidelberg, Germany.
52. Tran Van Nhieu, G., and Isberg, R. R. (1991) *J. Biol. Chem. 266*, 24367−24375.
53. Bennett, J. S., Kolodziej, M. A., Vilaire, G., and Poncz, M. (1993) *J. Biol. Chem. 268*, 3580−3585.
54. O'Shea, E. K., Rutkowski, R., Stafford, W. F., III, and Kim, P. S. (1989) *Science 254*, 646−648.
55. Kostelny, S. A., Cole, M. S., and Tso, J. Y. (1992) *J. Immunol. 148*, 1547−1553.
56. Chang, H.-C., Bao, Z.-Z., Yao, Y., Tse, A. G. D., Goyarts, E. C., Madsen, M., Kawasaki, E., Brauer, P. P., Sacchettini, J. C., Nathenson, S. G., and Reinherz, E. L. (1994) *Proc. Natl. Acad. Sci. U.S.A. 94*, 11408−11412.
57. Kalandadze, A., Galleno, M., Foncerrada, L., Strominger, J. L., and Wucherpfennig, K. W. (1996) *J. Biol. Chem. 271*, 20156−20162.
58. Delwel, G. O., Kuikman, I., Van der Schors, R. C., De Melker, A. A., and Sonnenberg, A. (1997) *Biochem. J. 324*, 263−272.
59. Leppa, S., Heino, J., and Jalkanen, M. (1995) *Cell Growth Differ. 6*, 853−861.
60. Haaparanta, T., Uitto, J., Rouslahti, E., and Engvall, E. (1991) *Matrix 11*, 151−160.
61. Miner, J. H., Lewis, R. M., and Sanes, J. R. (1995) *J. Biol. Chem. 270*, 28523−28526.
62. DiPersio, C. M., Shah, S., and Hynes, R. O. (1995) *J. Cell Sci. 108*, 2321−2336.
63. Berditchevski, F., Zutter, M. M., and Hemler, M. E. (1996) *Mol. Biol. Cell 7*, 193−207.
64. Nakamura, K., Iwamoto, R., and Mekada, E. (1995) *J. Cell Biol. 129*, 1691−1705.
65. Gailit, J., and Rouslahti, E. (1988) *J. Biol. Chem. 263*, 12927−12932.
66. Kirchhofer, D., Grzesiak, J., and Pierschbacher, M. D. (1991) *J. Biol. Chem. 266*, 4471−4477.
67. Mould, A. P., Akiyama, S. K., and Humphries, M. J. (1995) *J. Biol. Chem. 270*, 26270−26277.
68. Bazzoni, G., Ma, L., Blue, M.-L., and Hemler, M. E. (1998) *J. Biol. Chem. 273*, 6670−6678.
69. Pfaff, M., Göring, W., Brown, J. C., and Timpl, R. (1994) *Eur. J. Biochem. 225*, 975−984.
70. Jakubowski, A., Rosa, M. D., Bixler, S., Lobb, R., and Burkly, L. C. (1995) *Cell Adhes. Commun. 3*, 131−142.

BI980175+